

# Vibrational spectra of three new diarsenates containing scandium(III)

Enrique J. Baran,<sup>1\*</sup> Karolina Schwendtner<sup>2</sup> and Uwe Kolitsch<sup>2</sup>

<sup>1</sup> Centro de Química Inorgánica (CEQUINOR/CONICET, UNLP), Facultad de Ciencias Exactas, Universidad Nacional de La Plata, C. Correo 962, 1900 La Plata, Argentina

<sup>2</sup> Institut für Mineralogie und Kristallographie, Geozentrum, Universität Wien, Althansstr. 14, A 1090 Wien, Austria

Received 27 December 2005; Accepted 27 January 2006

**The powder Fourier transform (FT) infrared and Raman spectra of the new isotypic diarsenates RbScAs<sub>2</sub>O<sub>7</sub>, TlScAs<sub>2</sub>O<sub>7</sub>, and (NH<sub>4</sub>)ScAs<sub>2</sub>O<sub>7</sub> are discussed with a factor group analysis, on the basis of their known structural characteristics. The spectroscopic behavior clearly reflects all the structural peculiarities and also confirms the rotational quenching of the NH<sub>4</sub><sup>+</sup> cation in (NH<sub>4</sub>)ScAs<sub>2</sub>O<sub>7</sub>. The crystal structure of TlScAs<sub>2</sub>O<sub>7</sub> is also reported for the first time and is briefly discussed. Copyright © 2006 John Wiley & Sons, Ltd.**

**KEYWORDS:** diarsenates; vibrational spectra; factor group analysis

## INTRODUCTION

As part of a recently started study on the crystal chemistry of the Sc(III) cation in different oxygen environments, it was found that the double cation diarsenates, RbScAs<sub>2</sub>O<sub>7</sub> (Ref. 1), (NH<sub>4</sub>)ScAs<sub>2</sub>O<sub>7</sub> (Ref. 2), and TlScAs<sub>2</sub>O<sub>7</sub> (Ref. 3 and the present work), all belong to the KAlP<sub>2</sub>O<sub>7</sub> structural type<sup>3,4</sup> which is the most common type among M<sup>I</sup>M<sup>III</sup>P<sub>2</sub>O<sub>7</sub> diphosphates (see Ref. 1 for a brief review). Since they are the first diarsenates adopting this structure and since spectroscopic data of mixed cation diarsenates are extremely scarce, we have carried out a detailed investigation of their infrared and Raman spectra.

## EXPERIMENTAL

The three investigated compounds were obtained in high yields by hydrothermal syntheses, at 493 K, using a Teflon-lined stainless steel bomb, by reacting mixtures containing distilled water, Sc<sub>2</sub>O<sub>3</sub>, hydrated arsenic acid and Rb<sub>2</sub>CO<sub>3</sub>, ammonia, or Tl<sub>2</sub>CO<sub>3</sub>, respectively, for about one week.<sup>1,2</sup>

IR spectra in the range 4000–400 cm<sup>-1</sup> were recorded with a Bruker IF66 Fourier transform (FT) IR instrument using the KBr pellet technique. A total of 80 scans were accumulated at a nominal resolution of ±4 cm<sup>-1</sup>. Raman spectra in the range 4000–100 cm<sup>-1</sup> were measured on powdered samples using the FRA 106 Raman accessory of the same FTIR instrument (500 scans, nominal resolution

±4 cm<sup>-1</sup>). Radiation from a Nd:YAG solid-state laser (1064 nm) was used for excitation.

The previously unknown crystal structure of TlScAs<sub>2</sub>O<sub>7</sub> was determined from single-crystal X-ray diffraction data (293 K, CCD area detector). As input values for the structure model the positional parameters for isotypic RbScAs<sub>2</sub>O<sub>7</sub> were used.<sup>1</sup> The full-matrix least-squares anisotropic refinement led to a final residual *R*(*F*) of 2.28% (see Table 1 for details). The final positional and displacement parameters are given in Table 2 and selected bond distances in Table 3.

## RESULTS AND DISCUSSION

The three isotypic diarsenates crystallize in the monoclinic space group *P*2<sub>1</sub>/*c* (no.14) with four formula units (*Z* = 4) in the unit cell, and have very similar unit-cell parameters (Table 4). A polyhedral representation of the structure of TlScAs<sub>2</sub>O<sub>7</sub>, drawn with DIAMOND,<sup>6</sup> is shown in Fig. 1. The As<sub>2</sub>O<sub>7</sub><sup>4-</sup> diarsenate groups show a nearly staggered (*gauche*) conformation with As–O–As bridge angles near 120°, and all the atoms are located in general positions (Refs 1 and 2 and Tables 2 and 4). The conformation of the As<sub>2</sub>O<sub>7</sub> group in these diarsenates appears unusual because compounds with isolated X<sub>2</sub>O<sub>7</sub> groups (X=Si, P, S, As, Cr, Ge, and V) in general show either a staggered conformation, with a bridging X–O–X angle greater than 140° (up to 180°), or an eclipsed conformation, with an X–O–X angle of less than 140°, in which the O<sub>bridge</sub> atom belongs to the coordination sphere of at least one cation.<sup>7</sup>

As the anions present angular bridges and *gauche* conformation of their terminal groups, the symmetry of the 'free' anions is C<sub>1</sub>, coinciding with the site symmetry.<sup>8</sup>

\*Correspondence to: Enrique J. Baran, Centro de Química Inorgánica, Facultad de Ciencias Exactas, Universidad Nacional de La Plata, C. Correo 962, 1900 La Plata, Argentina.  
E-mail: baran@quimica.unlp.edu.ar

**Table 1.** Data collection information and refinement details for TlScAs<sub>2</sub>O<sub>7</sub>

Space group, <i>Z</i>	<i>P</i> 2 <sub>1</sub> / <i>c</i> (no. 14), 4
Wavelength	Mo–K $\alpha$ radiation (0.71073 Å)
$\mu$ (mm <sup>-1</sup> )	33.593
Diffractometer, scan mode	Nonius Kappa CCD, $\varphi/\omega$
2 $\theta_{\max}$	65
$N(hkl)_{\text{measured}}, N(hkl)_{\text{unique}}$	4922, 2519
Criterion for $I_{\text{obs}}, N(hkl)_{\text{gt}}$	$I_{\text{obs}} > 2\sigma(I_{\text{obs}})$ , 2356
$F(000), \delta_{\text{calc}}$ (g cm <sup>-3</sup> )	896, 4.889
$N(\text{param})_{\text{refined}}$	101
Extinction coefficient	0.00522(19)
GooF	1.055
$R1(F_{\text{obs}}), wR2(F_{\text{all}}^2)$	2.28%, 5.52%
Largest peak and hole (e Å <sup>-3</sup> )	1.92 and -2.17
Refinement program	SHELXL-97 <sup>5</sup>

**Table 2.** Atomic coordinates and displacement parameters of TlScAs<sub>2</sub>O<sub>7</sub>

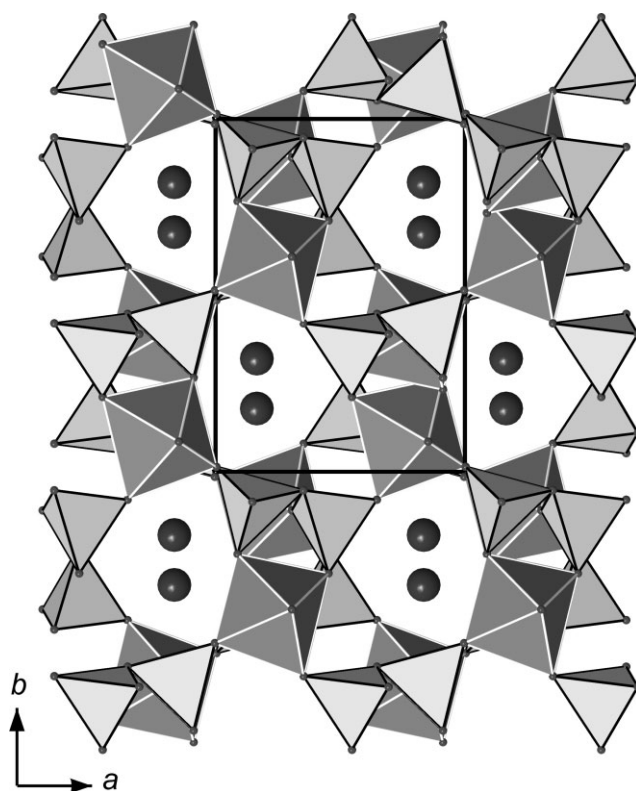
Atom	<i>x</i>	<i>y</i>	<i>z</i>	$U_{\text{equiv}}$
Tl	1.16539(2)	0.820734(18)	0.54906(2)	0.02765(7)
Sc	0.76382(7)	-0.90055(5)	0.73471(7)	0.00802(10)
As1	0.86032(4)	-0.59062(3)	0.66489(4)	0.00976(7)
As2	0.55634(4)	-0.86158(3)	0.30910(4)	0.00943(7)
O1	0.8526(5)	-0.9148(4)	0.9758(3)	0.0344(9)
O2	0.6937(5)	-0.8902(3)	0.4882(3)	0.0261(6)
O3	1.0030(3)	-0.9857(2)	0.7201(3)	0.0126(4)
O4	0.9118(3)	-0.7335(2)	0.7451(4)	0.0189(5)
O5	0.6469(4)	-1.0794(3)	0.7197(4)	0.0226(6)
O6	0.5470(3)	-0.7882(2)	0.7503(3)	0.0163(5)
O7	0.6471(3)	-0.9474(3)	0.1781(3)	0.0161(5)

**Table 3.** Selected bond lengths (Å) for TlScAs<sub>2</sub>O<sub>7</sub>

Tl–O3	2.823(2)	Sc–O1	2.027(3)
Tl–O4	2.888(3)	Sc–O2	2.068(3)
Tl–O6	3.025(3)	Sc–O5	2.095(3)
Tl–O4	3.101(3)	Sc–O4	2.105(3)
Tl–O3	3.119(3)	Sc–O6	2.107(3)
Tl–O5	3.272(3)	Sc–O3	2.112(2)
Tl–O2	3.307(3)	–	–
Tl–O5	3.335(3)	–	–
Tl–O1	3.429(5)	–	–
Tl–O7	3.451(3)	–	–
As1–O1	1.635(3)	As2–O2	1.657(3)
As1–O3	1.669(2)	As2–O5	1.659(3)
As1–O4	1.671(3)	As2–O6	1.666(3)
As1–O7	1.749(2)	As2–O7	1.759(2)

**Table 4.** Comparison of important crystallographic data of the three investigated compounds

	(NH <sub>4</sub> )ScAs <sub>2</sub> O <sub>7</sub>	RbScAs <sub>2</sub> O <sub>7</sub>	TlScAs <sub>2</sub> O <sub>7</sub>
<i>a</i> (Å)	7.842(2)	7.837(2)	7.814(2)
<i>b</i> (Å)	10.656(2)	10.625(2)	10.613(2)
<i>c</i> (Å)	8.765(2)	8.778(2)	8.726(2)
$\beta$ (°)	106.81(3)	106.45(3)	106.31(3)
<i>V</i> (Å <sup>3</sup> )	701.2(3)	701.0(3)	694.5(3)
As–O–As (°)	120.09(9)	119.62(10)	119.27(14)
References	2	1	This work

**Figure 1.** Polyhedral representation of the structure of TlScAs<sub>2</sub>O<sub>7</sub> seen along the *c* axis. As<sub>2</sub>O<sub>7</sub> diarsenate groups are corner-linked to slightly distorted ScO<sub>6</sub> octahedra. Ten-coordinate Tl<sup>+</sup> ions are located in tunnels running parallel to *c*. The unit cell is outlined.

The 21 internal vibrations are all of *A* symmetry. In order to perform the spectral analysis it seems adequate to use the factor group approximation to consider the coupling effects within the four As<sub>2</sub>O<sub>7</sub><sup>4-</sup> moieties present in the unit cell.<sup>8,9</sup> The correlation between the site group and the factor group is presented in Table 5, which also shows the distribution of the vibrational modes between the different symmetry species. As can be seen, the so-called mutual exclusion rule is operative, in agreement with the existence of an inversion center in the crystal structure; therefore, *g* modes

**Table 5.** Factor group analysis of the  $\text{As}_2\text{O}_7^{4-}$  vibrations in the investigated lattices ( $P2_1/c$  ( $C_{2h}^5$ ) and  $Z = 4$ )<sup>a</sup>

Vibrational mode	Site symmetry/ $C_1$	Factor group/ $C_{2h}$
Symmetric $\text{AsO}_3$ stretching	2A	$2A_g + 2B_g + 2A_u + 2B_u$
Antisymmetric $\text{AsO}_3$ stretching	4A	$4A_g + 4B_g + 4A_u + 4B_u$
Symmetric bridge stretching	A	$A_g + B_g + A_u + B_u$
Antisymmetric bridge stretching	A	$A_g + B_g + A_u + B_u$
Symmetric $\text{AsO}_3$ bending	2A	$2A_g + 2B_g + 2A_u + 2B_u$
Antisymmetric $\text{AsO}_3$ bending	4A	$4A_g + 4B_g + 4A_u + 4B_u$
Bridge bendings	4A	$4A_g + 4B_g + 4A_u + 4B_u$
Torsions	3A	$3A_g + 3B_g + 3A_u + 3B_u$

<sup>a</sup> Activity under factor group symmetry:  $A_g, B_g$ , Raman active;  $A_u, B_u$ , IR active.

are only Raman active, whereas  $u$ -modes show only IR activity.

Because of the fact that vibrational spectroscopic studies of crystalline diarsenates are relatively scarce, we have used the results from our previous studies of metal diarsenates<sup>10–14</sup> for the spectral analysis of the presently investigated compounds. In particular, the investigation of  $\text{PbCuAs}_2\text{O}_7$  is specially relevant,<sup>13</sup> as it represents a closely related diarsenate structure type.<sup>15</sup>

The internal vibrations of the  $\text{As}_2\text{O}_7^{4-}$  groups in the three compounds generate very similar spectral patterns, although the spectra of  $(\text{NH}_4)\text{ScAs}_2\text{O}_7$  shows a number of additional bands originating from the presence of the polyatomic  $\text{NH}_4^+$  cation. As an example of the recorded spectra, Fig. 2 shows the FTIR spectrum of  $\text{RbScAs}_2\text{O}_7$  in the spectral range between 1400 and 400  $\text{cm}^{-1}$ , and Fig. 3 shows the corresponding Raman spectrum up to 100  $\text{cm}^{-1}$ . The complete FTIR spectrum of  $(\text{NH}_4)\text{ScAs}_2\text{O}_7$  is shown in Fig. 4.

The assignment proposed for the IR and Raman spectra of  $\text{RbScAs}_2\text{O}_7$  and  $\text{TlScAs}_2\text{O}_7$  is shown in Table 6, whereas that of  $(\text{NH}_4)\text{ScAs}_2\text{O}_7$  is given in Table 7.

All spectra are very well defined showing nicely shaped bands, except in the Raman spectrum of  $(\text{NH}_4)\text{ScAs}_2\text{O}_7$ , which shows a relatively broad band in the region between 4000 and 1500  $\text{cm}^{-1}$ . This does not allow the location of the ammonium stretching vibrations, and the two deformational modes are seen only as weak bands on the decaying part of this broad feature. Besides, in all cases the number of observed bands is appreciably smaller than that predicted by the factor group analysis. This is a typical behavior usually found in solid-state spectra and is due to the fact that many

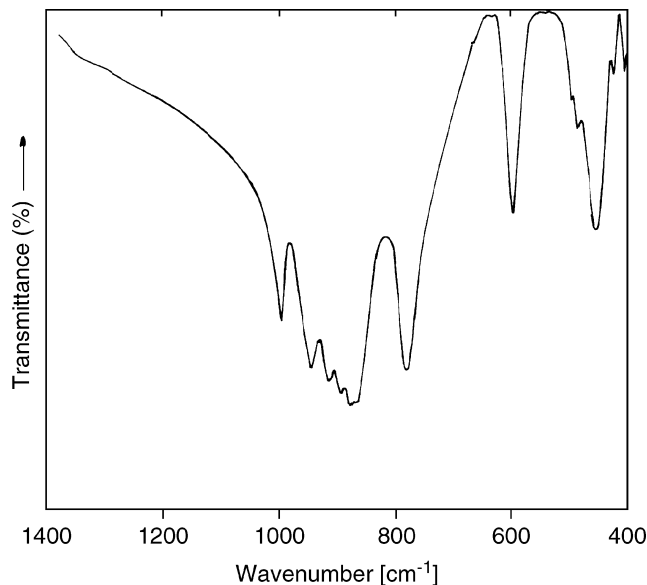


**Figure 2.** FTIR spectrum of  $\text{RbScAs}_2\text{O}_7$  in the spectral range 1400–400  $\text{cm}^{-1}$ .

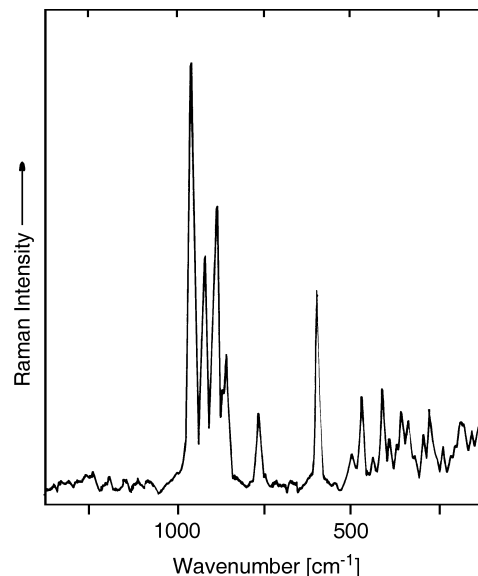


**Figure 3.** FT-Raman spectrum of  $\text{RbScAs}_2\text{O}_7$  in the spectral range 1400–100  $\text{cm}^{-1}$ .

of the theoretically predicted bands may lie close together and, as a consequence of this accidental degeneracy, they appear overlapped in the spectra.

On the basis of a more detailed analysis of the observed  $\text{As}_2\text{O}_7^{4-}$  vibrations in the three investigated compounds, the following comments are made:

- In all cases, the symmetric stretching vibration of the terminal  $\text{AsO}_3$  groups generates a unique IR and Raman band. This vibration corresponds to the strongest band in the Raman spectra of the Rb and Tl compounds. One of the  $\nu_{\text{as}}(\text{AsO}_3)$  components of  $(\text{NH}_4)\text{As}_2\text{O}_7$  (at 888  $\text{cm}^{-1}$ ) is

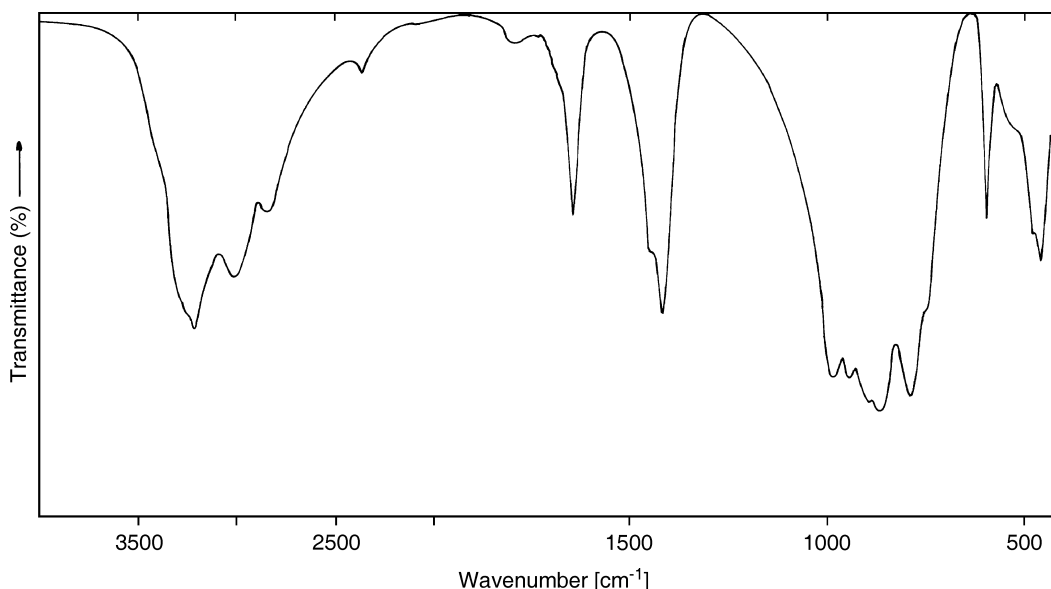


**Figure 4.** FTIR spectrum of  $\text{NH}_4\text{ScAs}_2\text{O}_7$  in the spectral range  $4000\text{--}400\text{ cm}^{-1}$ .

**Table 6.** Wavenumbers and assignment of the vibrational spectra of  $\text{RbScAs}_2\text{O}_7$  and  $\text{TlScAs}_2\text{O}_7$ <sup>a</sup>

$\text{RbScAs}_2\text{O}_7$		$\text{TlScAs}_2\text{O}_7$		Assignment
IR, $\nu$ ( $\text{cm}^{-1}$ )	Raman, $\nu$ ( $\text{cm}^{-1}$ )	IR, $\nu$ ( $\text{cm}^{-1}$ )	Raman, $\nu$ ( $\text{cm}^{-1}$ )	
995 s	981 vs	985 m	956 vs	$\nu_s(\text{AsO}_3)$
943 s	–	935 s	916 s	–
912 m	920 s	908 m	884 vs	$\nu_{as}(\text{AsO}_3)$
886 m	885 vs	880 sh	–	–
877 vs, 853 vs	870 sh, 859 m	866 vs	858 m	–
779 vs	771 w	781 vs	764 w	$\nu_{as}(\text{As–O–As})$
594 vs	598 vs	596 vs	598 s	$\nu_s(\text{As–O–As})$
520 sh, 502 sh	494 vw	472 sh	465 sh	–
449 vs	466 m	–	459 m	$\delta_{as}(\text{AsO}_3)$
418 vw, 405 w	426 vw, 405 m	438 vs	418 s	–
–	380 w, 355 sh	–	398 m	$\delta_s(\text{AsO}_3)$
–	349 w, 322 w	–	348 m, 327 m	–
–	279 w	–	283 w	–
–	265 w	–	263 w	See text
–	224 w, 178 w	–	226 w, 181 w	–

<sup>a</sup> vs, very strong; s, strong; m, medium; w, weak; vw, very weak; sh, shoulder.

somewhat stronger. The energy of this symmetric vibration is similar in all cases.

- The splitting of the antisymmetric stretching mode of the terminal groups generates a similar pattern in all cases, but the number of components is not the same in the three compounds. In  $\text{RbScAs}_2\text{O}_7$  five of the eight expected IR and four of the eight expected Raman components are observed. In the other two compounds this number is smaller. However, the expected site symmetry components are at least evident. Also, these vibrations are found in very similar ranges in all the cases.

- The As–O–As bridge vibrations are also found in similar energy ranges in the three cases. This is in excellent agreement with the similar values of the bridge angles in these diarsenates ( $\sim 120^\circ$ , Table 4). The measured wavenumbers are also comparable to those reported<sup>13</sup> for  $\text{PbCuAs}_2\text{O}_7$  ( $\nu_s = 586$ ,  $\nu_{as} = 777\text{ cm}^{-1}$ ), which presents<sup>15</sup> bridge angles of about  $124^\circ$ . Only in the case of  $\text{TlScAs}_2\text{O}_7$  the corresponding antisymmetric vibration shows the predicted factor group splitting. In the other cases only one band is seen for each of these modes. Both bridge vibrations are relatively strong in the IR spectrum, whereas in the

**Table 7.** Wavenumbers and assignment of the vibrational spectra of  $\text{NH}_4\text{ScAs}_2\text{O}_7^{\text{a}}$ 

IR, $\nu$ ( $\text{cm}^{-1}$ )	Raman, $\nu$ ( $\text{cm}^{-1}$ )	Assignment
3310 sh, 3209 vs	–	$\nu_3(\text{NH}_4^+)$
3003 m	–	$\nu_1(\text{NH}_4^+)$
2849 w	–	$2\nu_4(\text{NH}_4^+)$
2362 vw	–	(?) see text
1796 vw	–	$\nu_4 + \nu_6(\text{NH}_4^+)$ see text
1645 s	1605 w	$\nu_2(\text{NH}_4^+)$
1440 sh, 1419 vs	1403 w	$\nu_4(\text{NH}_4^+)$
985 vs	965 vs	$\nu_5(\text{AsO}_3)$
945 s, 899 m, 860 vs	933 s, 888 vs, 866 m	$\nu_{\text{as}}(\text{AsO}_3)$
–	834 m	–
787 vs, 754 sh	804 m, 765 m	$\nu_{\text{as}}(\text{As-O-As})$
594 s	597 s	$\nu_5(\text{As-O-As})$
540 sh, 478 sh, 457 s,	542 w, 504 vw,	$\delta_{\text{as}}(\text{AsO}_3)$
414 sh	471 m, 437 w, 400 w	
–	360 vw, 347 m,	$\delta_s(\text{AsO}_3)$
–	283 w, 269 vw, 243 w	See text

<sup>a</sup> vs, very strong; s, strong; m, medium; w, weak; vw, very weak; sh, shoulder.

Raman spectrum the symmetric mode is always stronger than the corresponding antisymmetric one, as expected.

- The assignment of the  $\text{AsO}_3$  deformational modes is more difficult, especially in the lower wavenumber range, as in this region external (lattice) vibrations are expected and probably an important coupling between internal and external modes may occur. Notwithstanding this, in all cases, we have assigned the block of IR bands centered at about  $440\text{--}460\text{ cm}^{-1}$  to the  $\delta_{\text{as}}(\text{AsO}_3)$  components. The next group of bands, recorded only in the respective Raman spectra, were assigned, tentatively, to components of the corresponding symmetric deformational mode.
- In all cases, the last group of weak Raman lines can be assigned to external modes.
- The position of the As–O–As bending vibration could not be established with certainty. But in agreement with the information available for other  $\text{X}_2\text{O}_7$  systems,<sup>8,16–20</sup> it probably lies below  $200\text{ cm}^{-1}$ .
- It is well known that the Tl(I) cation usually has a strong impact on the vibrational modes of oxoanions producing important shifts to lower energies, due to the generation of weak covalent Tl–O interactions.<sup>9,21</sup> In the present case, these effects become only partially evident, if one compares the stretching vibrations of the terminal  $\text{AsO}_3$  groups of the Rb and Tl diarsenates.
- It is also interesting to note that in the three investigated compounds the corresponding IR and Raman bands generally appear at different wavenumbers, in agreement with the different phononic origins of the respective vibrations.

These energy differences are usually considered as a valuable criterion for the evaluation of the strength of coupling effects in the unit cell,<sup>22,23</sup> and in the present cases show that these effects are relatively weak.

A detailed analysis of the  $\text{NH}_4^+$  vibrations in  $(\text{NH}_4)\text{ScAs}_2\text{O}_7$  shows also some remarkable aspects. Both the antisymmetric stretching ( $\nu_3$ ) and bending ( $\nu_4$ ) vibrations are clearly split in the IR spectrum, whereas the symmetric stretching vibration ( $\nu_1$ ) is also present as a medium-intensity IR band. Moreover, the symmetric deformational ( $\nu_2$ ) band is also relatively intense.

The splitting of the triply degenerate vibration modes ( $\nu_3$  and  $\nu_4$ ), together with the activation of some combinational and overtone modes, is usually regarded as a proof that the  $\text{NH}_4^+$  cation does not rotate freely in the lattice,<sup>24–26</sup> as is the case in the investigated compound here, for which all hydrogen atoms could be located during the crystal structure analysis.<sup>2</sup> One of the expected overtones is clearly seen as a weak band at  $2849\text{ cm}^{-1}$ , which can be assigned to  $2\nu_4$ . The weak and broad feature at about  $1790\text{ cm}^{-1}$  may be related to one of the expected combinations involving  $\nu_4$  and an external (lattice) mode located at about  $360\text{ cm}^{-1}$  ( $\nu_4 + \nu_6$  in Waddington's nomenclature<sup>24</sup>). The other usually observed combinational mode ( $\nu_2 + \nu_4$ ) is expected at around  $3070\text{ cm}^{-1}$  and is probably overlapped by the strong  $\nu_3/\nu_1$  feature (Fig. 4).

Finally, the weak IR band found at  $2362\text{ cm}^{-1}$  cannot be assigned with certainty. It probably is also a combinational or overtone mode, involving diarsenate or diarsenate/ammonium modes.

To conclude, the results of the spectroscopic analysis are in excellent agreement with the structural features of this new diarsenate series because (1) they reflect the overall geometrical and bond properties of the  $\text{As}_2\text{O}_7^{4-}$  anions, (2) they confirm the isotopic nature of the three compounds, and (3) they demonstrate the inhibition of free rotation of the ammonium cation in  $(\text{NH}_4)\text{ScAs}_2\text{O}_7$ .

## Acknowledgements

This work was supported by the Consejo Nacional de Investigaciones Científicas y Técnicas de la República Argentina (CONICET), DOCFFORTE (Frauen in Forschung und Technologie) of the Austrian Academy of Sciences (ÖAW), the Austrian Science Foundation (FWF), and the International Centre for Diffraction Data (Grant 90-03 ET). E.J.B. is a member of the Research Career from CONICET and K.S. is a DOC-FFORTE fellow.

## REFERENCES

1. Schwendtner K, Kolitsch U. *Acta Crystallogr., Sect. C* 2004; **60**: i79.
2. Kolitsch U. *Z. Kristallogr.* 2004; **219**: 207.
3. Ng NH, Calvo C. *Can. J. Chem.* 1973; **51**: 2613.
4. Durif A. *Crystal Chemistry of Condensed Phosphates*. Plenum Press: New York, 1995.
5. Sheldrick GM. *SHELXL-97, Program for Crystal Structures Analysis*. University of Göttingen: Göttingen, 1997.

6. Brandenburg K. *DIAMOND*. Crystal Impact GbR: Bonn, 2005.
7. Clark GM, Morley R. *Chem. Soc. Rev.* 1976; **5**: 269.
8. Ross SD. *Inorganic Infrared and Raman Spectra*. McGraw-Hill: London, 1972.
9. Müller A, Baran EJ, Carter RO. *Struct. Bonding* 1976; **26**: 81.
10. Baran EJ, Pedregosa JC, Aymonino PJ. *J. Mol. Struct.* 1974; **22**: 377.
11. Botto IL, Baran EJ, Aymonino PJ, Pedregosa JC, Puelles G. *Monatsh. Chem.* 1975; **106**: 1559.
12. González-Baró AC, Baran EJ, Nord AG. *An. Asoc. Quím. Argent.* 1988; **76**: 121.
13. Baran EJ, Etcheverry SB. *An. Asoc. Quím. Argent.* 1988; **76**: 397.
14. Baran EJ, Weil M. *J. Raman Spectr.* 2004; **35**: 178.
15. Pertlik F. *Monatsh. Chem.* 1986; **117**: 1343.
16. Mathur MS, Frenzel CH, Bradley EB. *J. Mol. Struct.* 1968; **2**: 429.
17. Beattie JR, Ozin GA. *J. Chem. Soc. A* 1969; 2615.
18. Mattes R, Königer F, Müller A. *Z. Naturforsch.* 1974; **29b**: 58.
19. Baran EJ. *J. Mol. Struct.* 1978; **48**: 441.
20. Baran EJ, Botto IL, Pedregosa JC, Aymonino PJ. *Monatsh. Chem.* 1978; **109**: 41.
21. Baran EJ, Aymonino PJ, Müller A. *Z. Naturforsch.* 1969; **24b**: 271.
22. Müller A. *Z. Naturforsch.* 1966; **21a**: 433.
23. Baran EJ, Ferrer EG, Bueno I, Parada C. *J. Raman Spectr.* 1990; **21**: 27.
24. Waddington TC. *J. Chem. Soc.* 1958; 4340.
25. Mathieu JP, Poulet H. *Spectrochim. Acta* 1960; **16**: 696.
26. Baran EJ, Aymonino PJ. *Z. Anorg. Allg. Chem.* 1967; **354**: 85.